Energy Proceedings
Vol 46, 2024
ISSN 2004-2965

# Preparation and Simulation of 3D Printed Cu/ZnO Structured Catalysts for On-Board Methanol Steam Reforming

Chuandong Li [1], Hongxiang Zheng [1], Ruhang Zhang [1], Xinhai Yu [1*], Bo Li [2], Shan-Tung Tu [1]

1 Key Laboratory of Pressure Systems and Safety (MOE), School of Mechanical and Power Engineering, East China University of Science and Technology, Shanghai, 200237, China

2 Additive Manufacturing and Intelligent Equipment Research Institute, School of Mechanical and Power Engineering, East China University of Science and Technology, Shanghai 200237, China
(*Corresponding Author: yxhh@ecust.edu.cn)

**ABSTRACT**

Currently, the main types of methanol steam reforming (MSR) reactors used in vehicles are fixed bed reactors and microchannel reactors. However, these two-dimensional reactors have limitations such as restricted radial diffusion, catalyst coating peeling off easily, and high pressure drop. In this study, a new type of three-dimensional porous Cu/ZnO catalyst was developed using 3D printing combined with dealloying technology. The internal mass and heat transfer characteristics of the three catalyst structures, Cylindrical microchannel, Diamond, and Gyroid, were revealed using computational fluid dynamics (CFD) simulation. The simulation results showed that the Gyroid structure with its curved and smooth flow channels enhanced radial mass and heat transfer while having the advantage of low pressure drop. Performance tests showed that the Gyroid structure catalyst exhibited high activity and good stability.

**Keywords:** methanol steam reforming, laser powder bed fusion, dealloying, structural catalyst, computational fluid dynamics

**NONMENCLATURE**

| | |
|---|---|
| *Abbreviations* | |
| MSR | Methanol steam reforming |
| SMSI | Strong metal–support interaction |
| CFD | Computational fluid dynamics |
| 3D | Three-dimensional |
| SR | Steam reforming |
| rWGS | Reverse water-gas shift |
| WGS | Water-gas shift |
| *WHSV* | Weight hourly space velocity |
| *Symbols* | |
| $p_A$ | Absolute pressure |
| $u$ | Velocity field |
| $\mu$ | Dynamic viscosity |
| I | Identity matrix |
| $T$ | Viscous stress tensor |
| $C_p$ | Heat capacity |
| $E_1$, $E_2$, *and* $E_3$ | Activation Energy of SR, rWGS, and WGS Reactions |
| $K_1$, $k_2$ and $k_3$ | Pre-exponential factors for SR, rWGS, and WGS reactions |

## 1. INTRODUCTION

Hydrogen, as a clean energy source, is considered an ideal alternative to fossil fuels. Fuel cells can convert hydrogen into electricity, providing a wide range of applications for electric vehicles [1]. However, the high cost of hydrogen production and safety concerns related to direct hydrogen storage have hindered the development of hydrogen-powered vehicles [2]. Methanol steam reforming (MSR) technology for on-board hydrogen production can reduce the cost of hydrogen production and ensure safety during vehicle operation [3]. The key to MSR is the development of efficient catalysts and reactors [4]. Currently, commercial particulate $Cu/ZnO/Al_2O_3$ catalysts used in fixed-bed reactors face issues such as high pressure drop and poor mass and heat transfer performance [5]. Yu et al. [6] used mechanical micro-cutting technology to fabricate a parallel microchannel integrated MSR reactor, which achieved high hydrogen production efficiency and provided 10W of power. Liu et al. [7] developed an ordered pore array of three-dimensional

# This is a paper for 15th International Conference on Applied Energy (ICAE2023), Dec. 3-7, 2023, Doha, Qatar.

(3D) Cu foam as a porous support for Cu/Zn/Al/Zr catalysts. Test results showed that the ordered pore structure improved methanol conversion. Although 3D catalyst supports demonstrate significant advantages in mass and heat transfer, the use of coating or impregnation processes to load catalysts introduces the risk of catalyst peeling, which can contaminate the MSR reaction system.

Through the utilization of 3D printing and dealloying techniques, catalysts with hierarchical porous structures can be fabricated, enabling the design of intricate architectures that provide a high specific surface area and enhance catalyst loading [8]. The lattice structure hierarchical nano Cu catalyst prepared using 3D printing and dealloying technology exhibited high methanol conversion rates [9]. However, the use of single Cu as a catalyst has drawbacks such as high reaction temperatures and susceptibility to sintering. Furthermore, the impact of different types of 3D printed porous structures on MSR reaction performance has not been extensively studied. To address these issues, this study developed Cu/ZnO structured catalysts for on-board MSR reactions using 3D printing and dealloying technology. Computational Fluid Dynamics (CFD) simulation was employed to analyze the mass and heat transfer characteristics of three different catalyst structures: Cylindrical microchannel, Diamond, and Gyroid. The study also aimed to reveal the influence of porous structure shapes on MSR reaction performance.

## 2. EXPERIMENTS AND METHODS

### *2.1 Preparation of structural catalysts*

A 3D printed spherical powder with a nominal composition of 50Al45Cu5Zn (wt. %) was prepared using gas atomization pre-alloying technique. The printing parameters are as follows: laser power of 230-260W, scanning speed of 900 m $s^{-1}$, and powder layer thickness of 45μm. A 90° interlayer scanning strategy was adopted to improve sintering strength and prevent the formation of micro-cracks induced by thermal stress. The three different structure catalysts, namely Cylindrical microchannel (Type-1), Diamond (Type-2), and Gyroid (Type-3), had a length of 50mm and a diameter of 25mm, with more specific dimensions shown in Fig. 1.

Chemical dealloying process was utilized to create surface nano-porous structures on the catalysts. The printed substrates were immersed in a 1mol $L^{-1}$ KOH aqueous solution for 6 h to remove the surface Al elements in the alloy. The dealloyed catalyst were then rinsed multiple times in ultrapure water, followed by drying for 24 h. Finally, the samples were annealed at 450 °C for 3 h to enhance the structural strength of the surface nano-porous Cu/ZnO catalysts. The 3D printed catalyst structures were activated for 1 h at 10% $H_2/N_2$ and 300 °C for activity testing.

### *2.2 CFD simulation method*

#### 2.2.1 Physical model and calculation domain of reactor

The three different structure catalysts were designed using commercial implicit modeling software nTopology, and they were obtained through unit cell arrays, with the unit cell dimensions shown in Fig. 1. The surface area of Type-3 structure was 2.02 times that of Type-1. A computational fluid domain (green region) extended 20 mm on both sides to simulate the flow of gas-phase components in the metallic tube reactor. The left side of the fluid domain was set as the velocity inlet boundary condition with a velocity of $v$=0.2 m $s^{-1}$, while the right

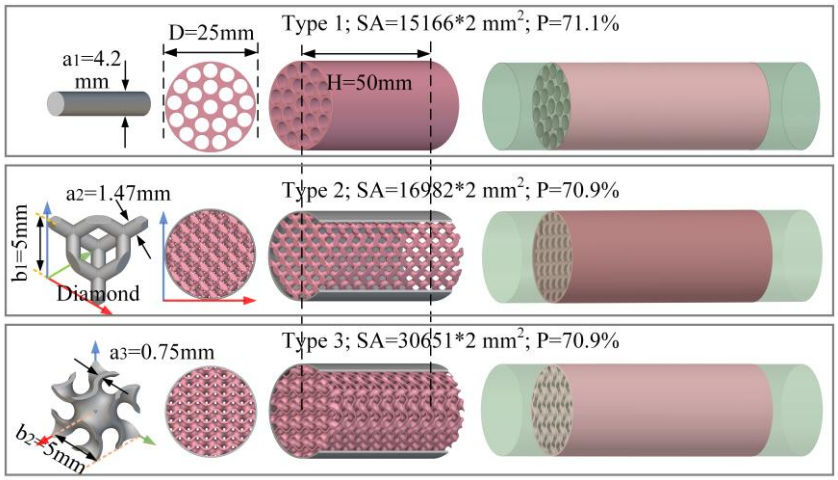


Fig. 1. Geometrical schematic diagram of 3D printed Type-1, Type-2, Type-3 structure catalysts with corresponding fluid computational domains

side was set as the pressure outlet with a pressure of *P*=0 Pa. The surroundings of the fluid domain were set as the wall for heat transfer, with a temperature of *T*=280 °C. The catalyst surface was set as the wall for reaction. The number of meshes divided for the three types of structural catalysts was 2803727, 4900637, and 6971547 respectively.

2.2.2 Mathematical model of the calculation domain

Continuity and momentum equations:

$$\nabla \cdot (\rho u) = 0 \quad (1)$$

$$\rho(u \cdot \nabla)u = \nabla \cdot [-pI + K] + F \quad (2)$$

where $\rho = \frac{p_A}{R_S T}$, $p_A$ is the absolute pressure, $u$ is the velocity field. $K = \mu(\nabla u + (\nabla u)^T) - \frac{2}{3}\mu(\nabla \cdot u)I$, where $\mu$ is dynamic viscosity, I is the identity matrix, $F$ is the volume force generated by gravity, $F$=0.

Energy conservation equation:

$$\rho C_p u \cdot \nabla T + \nabla \cdot q = Q + Q_p + Q_{vd} \quad (3)$$

Where $q = -k\nabla T$, $C_p$ is the constant pressure heat capacity for fluid, $Q_p = \alpha_p T\left(\frac{\partial p_A}{\partial t} + u \cdot \nabla p_A\right)$, $\alpha_p = -\frac{1}{\rho}\left(\frac{\partial \rho}{\partial T}\right)_p$, $Q_{vd} = \tau : \nabla u$, $\tau$ is the viscous stress tensor.

Heat transfer equation：

$$\rho C_p u \cdot \nabla T + \nabla \cdot q = Q + Q_{ted} \quad (4)$$

Where $q = -k\nabla T$, $\rho$ is the material density, $k$ is the thermal conductivity, $C_p$ heat capacity at constant pressure.

The kinetic model of the MSR reaction consists of three chemical reactions, as shown in Eqs. (5) to (7):

Steam reforming (SR):

$$CH_3OH + H_2O \rightarrow 3H_2 + CO_2 \quad \Delta H_{SR} = 49.4\ \text{kJ/mol} \quad (5)$$

Decomposition (DE):

$$CH_3OH \rightarrow CO_2 + 2H_2 \quad \Delta H_{DE} = 90.5\ \text{kJ/mol} \quad (6)$$

Reverse water gas shift (rWGS):

$$CO_3 + H_2 \rightleftharpoons HO_2 + CO \quad \Delta H_{rWGS} = 41.4\ \text{kJ/mol} \quad (7)$$

The dual-rate model proposed by Hu et al [10] for the SR and rWGS reactions was used to simulate the MSR reaction of 3D printed nanoporous Cu/ZnO catalysts as shown in Eqs. (8) and (9).

$$R_{SR} = k_1 e^{-E_1/RT} C_{CH_3OH}^{0.6} C_{H_2O}^{0.4} \quad (8)$$

$$R_{rWGS} = k_2 e^{-E_2/RT} C_{CO_2} C_{H_2}\left(1 - \frac{1}{K_{rWGS}}\frac{C_{H_2O}C_{CO}}{C_{CO_2}C_{H_2}}\right), K_{rWGS} = e^{E_{WGS}/RT - k_{WGS}} \quad (9)$$

$E_1$ and $k_1$ represent the reaction activation energy and pre-exponential factor for the steam reforming (SR) reaction, while $E_2$ and $k_2$ represent the activation energy and pre-exponential factor for the reverse water-gas shift (rWGS) reaction. $E_{WGS}$ and $k_{WGS}$ represent the activation energy and pre-exponential factor for the WGS reaction. $C$ denotes the concentration of the gas, with superscripts indicating reaction orders and subscripts indicating the corresponding component.

The apparent activation energy and pre-exponential factor for the MSR reaction were obtained through linear regression and are presented in Table 1 as follows:

**Table 1** Values of pre-exponential factor and activation energy for SR, rWGS and WGS reactions

| | SR, $k_1$ | SR, $E_1$ (kJ mol$^{-1}$) | rWGS, $k_2$ | rWGS, $E_2$ (kJ mol$^{-1}$) | WGS, $k_3$ | WGS, $E_3$ (kJ mol$^{-1}$) |
|---|---|---|---|---|---|---|
| Type-1 | $6.9\times10^8$ | 80 | $5.1\times10^9$ | 112 | $3.6\times10^7$ | 68 |
| Type-2 | $8.7\times10^8$ | 76 | $6.6\times10^9$ | 108 | $4.1\times10^7$ | 67 |
| Type-3 | $9.5\times10^8$ | 73 | $7.7\times10^9$ | 93 | $5.4\times10^7$ | 64 |

*2.3 Catalytic activity evaluation*

The MSR reaction on the structured catalysts was conducted in a stainless steel tube with a length of 200 mm and an inner diameter of 25 mm. Gas pipelines were connected to the flange faces at both ends of the metal tube. Thermocouples were installed inside and outside the metal tube to control the reaction temperature. Methanol-water solution was gasified in the heater under the action of a flow pump, and the gasified methanol steam entered the metal tube reactor for steam reforming reaction. The gas composition of the reaction gas was detected in a gas chromatograph (GC-8890) equipped with a thermal conductivity detector (TCD) and a flame ionization detector (FID). The calculation of methanol conversion rate, CO selectivity, and $H_2$ yield is shown in equations (10) –(12):

$$X_{CH_3OH}(\%) = \frac{(F_{CO,out} + F_{CO_2,out})}{F_{CH_3OH,in}} \times 100\% \quad (10)$$

$$S_{CO}(\%) = \frac{F_{CO,out}}{F_{CO,out} + F_{CO_2,out}} \times 100\% \quad (11)$$

$$Y_{H_2}(\%) = \frac{F_{H_2,out}}{3 \times F_{CH_3OH,in}} \times 100\% \quad (12)$$

where $F$ is the molar flow rates of the detected gas, the first subscript indicates the gas component, and the second indicates the input or output.

## 3. RESULTS AND DISCUSSION

### *3.1 CFD simulation*

#### 3.1.1 $H_2$ concentration field distribution of the structural reactors

As shown in Fig. 2, the concentration of $H_2$ in the three types of catalysts gradually increases with the increase of Z-axis distance and reaches its maximum at the outlet, with values of 30.2%, 65.5%, and 71.5% respectively. The Type-3 structure, characterized by a larger surface area and S-shaped curved channels, increases the contact time between reactants and the surface of the bimetallic catalyst, thereby enhancing the conversion rate of methanol and resulting in higher $H_2$ concentration. Compared to simulated results of commercial packed pellet catalysts [11], the radial distribution of $H_2$ in the 3D-printed structured catalyst is more uniform. This is attributed to the interconnected lattice array with uniform pore distribution, facilitating the transport and diffusion of reactants. It can be observed that the radial distribution uniformity of $H_2$ in the Type-3 structure outperforms that of the Type-2 structure. Additionally, in contrast to the straight channels in Type-1, the non-straight channels in Type-2 and Type-3 disrupt the flow of fluid in the same direction, thereby accelerating the transport of reactants and products. This effect is more pronounced in the Type-3 structure, particularly due to its spiral surface.

#### 3.1.2 Study of pressure drop, temperature and flow rate distribution in structural reactors

As shown in Fig. 3(a), the pressure drop for the three structures of catalysts decreases linearly with increasing distance of fluid into the reformer from 20 mm to 70 mm. When the inlet velocity is 0.2 m $s^{-1}$, the pressure drops at the inlet of Type-3, Type-2, and Type-1 structures are 14.5 Pa, 7.96 Pa, and 1.04 Pa, respectively. The temperature of methanol water vapor shows a continuous increase after coming into contact with the structured catalyst at Z=20 mm, as depicted in Fig. 3(b). Type-3, Type-2, and Type-1 reach the reaction temperature (heat source temperature) of 553 K at distances of 41 mm, 56 mm, and 70 mm, respectively. It is evident that Type-3 achieves the highest temperature in the shortest distance, highlighting its superior heat transfer efficiency. The commercial $Cu/ZnO/Al_2O_3$ catalysts have a radial heat distribution with lower temperatures at the center and higher temperatures at the edges, leading to a significant temperature difference [9]. This is due to the lower thermal conductivity of the catalyst material. It is evident that the axial temperature distribution curve of the Type-3 structure is smoother compared to that of the Type-2 structure. This indicates that the gas mixture entering

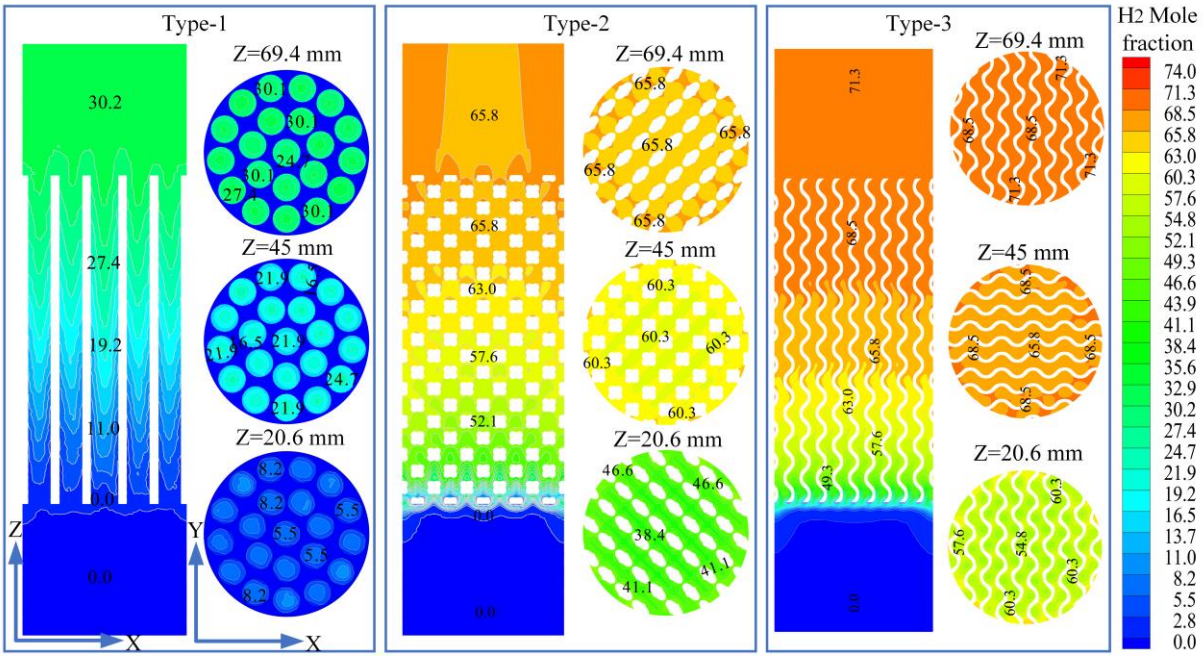


Fig. 2. Simulation results of the $H_2$ concentration distribution for the three structured catalysts in the metal tube reactor, including the distribution along the axial cross-section and the radial cross-section at Z=20.6, 45, and 69.4 mm, respectively. (Reaction conditions: inlet flow rate: 0.2 m $s^{-1}$, S/C ratio= 1.3, inlet temperature: 373 K, external wall temperature is 553 K)

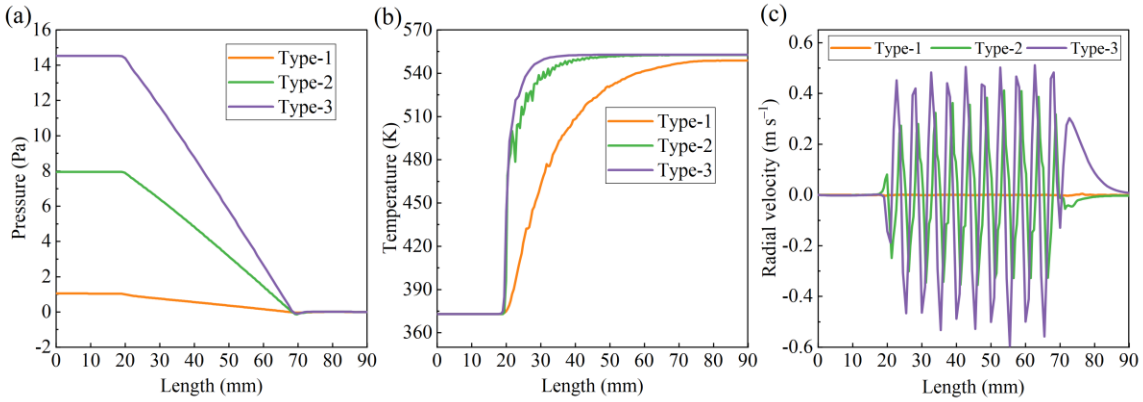


Fig. 3. Variation of pressure drop (a) and temperature (b) along the distance from the central axis for the three structures of catalysts. (c) The radial flow velocity distribution along the distance from the central axis for the three structures of catalysts. (Reaction conditions: inlet flow rate 0.2 m $s^{-1}$, S/C ratio= 1.3, inlet temperature is 373 K, external wall temperature is 553 K)

the Type-3 structure is more stable and uniform, leading to a significant improvement in the performance of Type-3 in terms of methanol conversion and hydrogen production rate. In comparison, the uneven heat distribution in packed bed reactors containing granular and powdered catalysts can lead to cold spots and hot spots, resulting in reduced reaction efficiency [12]. From Fig. 3(c), it can be observed that the radial velocity component of Type-1 is almost zero, while Type-2 and Type-3 structures exhibit periodic variations in radial velocity. Furthermore, Type-3 possesses a more uniform radial velocity distribution and can reach a maximum value of −0.6 m $s^{-1}$, which is approximately 50% higher than that of Type-2. This indicates that the Type-3 structure has a higher radial transport capability.

### *3.2 Performance of structural catalysts*

The performance test results of the 3D printed structure catalysts in the MSR process are shown in Fig. 7. As shown in Fig. 4(a), the methanol conversion rate, $H_2$ yield, and CO selectivity of the Type-1, Type-2, and Type-3 structure catalysts increase continuously as the temperature rises from 240 °C to 310 °C. Among them, the Type-3 structure catalyst exhibits the best catalytic performance, with a methanol conversion rate of 95.5%, $H_2$ yield of 94.1%, and CO selectivity of 0.83% at 280 °C. As shown in Fig. 4(b), the Type-3 structure shows a higher $H_2$ concentration of 74.6%, which is 2.33 times that of the Type-1 structure. The $H_2$ concentration of the three structure catalysts is close to the simulated results, indicating the accuracy of the dual-rate model.

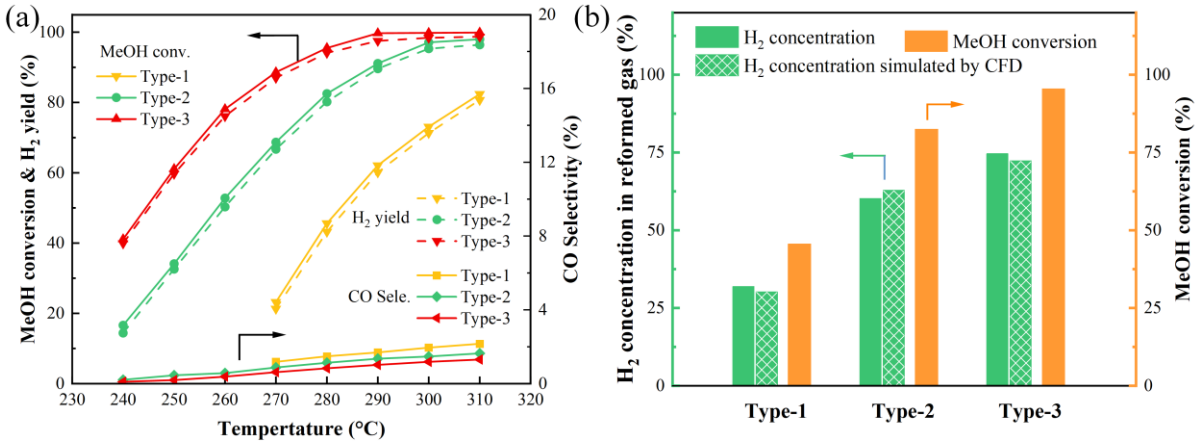


Fig. 4. (a) Variation of MeOH conversion, $H_2$ yield, and CO selectivity with temperature for Type-1, Type-2, and Type-3 structure catalysts. Reaction conditions: WHSV=30 $h^{-1}$, S/C=1.3. (b) Comparison of methanol conversion rates for Type-1, Type-2, and Type-3 structure catalysts. Reaction conditions: WHSV=30 $h^{-1}$, S/C=1.3, T=280 °C. Comparison of $H_2$ concentration in the reforming gas and simulated $H_2$ concentration. Inlet velocity v=0.2 m/s, S/C=1.3, T=280 °C.

## 4. CONCLUSIONS

Nanoporous Cu/ZnO catalysts with three-dimensional structures, namely Cylindrical microchannel, Diamond, and Gyroid, were successfully prepared by combining LPBF 3D printing technology with dealloying. The nanoscale Cu particles were encapsulated with ZnO, which enhanced the interaction between the strong metal support and increased the number of active $Cu^+$ centers. The catalytic evaluation experiments showed that the Type-3 structure exhibited a higher methanol conversion rate of 95.5% and a lower CO selectivity of 0.83%. CFD simulation results demonstrated that the Type-3 structure catalyst possessed excellent heat transfer performance and a higher $H_2$ concentration. This was attributed to the smooth and curved flow channels in the Gyroid structure, which enhanced mass and heat transfer, thereby improving the catalytic performance.


## ACKNOWLEDGMENT

This study was financially supported by China Natural Science Foundation (Contract No. 21176069).


## DECLARATION OF INTEREST STATEMENT

The authors declare that they have no known competing financial interests or personal relationships that could have appeared to influence the work reported in this paper. All authors read and approved the final manuscript.

## REFERENCE


[1] Nikolaidis P, Poullikkas A. A comparative overview of hydrogen production processes. Renew Sustain Energy Rev 2017;67:597-611.

[2] Yu W, Tao J, Yu X, Zhao S, Tu S, Liu H. A microreactor with superhydrophobic Pt-$Al_2O_3$ catalyst coating concerning oxidation of hydrogen off-gas from fuel cell. Appl Energy 2017;185:1233-44.

[3] Bepari S, Kuila D. Steam reforming of methanol, ethanol and glycerol over nickel-based catalysts-A review. Int J Hydrogen Energ 2020;45:18090-113.

[4] Yu XH, Tu ST, Wang ZD, Qi YS. On-board production of hydrogen for fuel cells over Cu/ZnO/$Al_2O_3$ catalyst coating in a micro-channel reactor. J Power Sources 2005;150:57-66.

[5] Düsterwald H, Höhlein B, Kraut H, Meusinger J, Peters R, Stimming U. Methanol steam-reforming in a catalytic fixed bed reactor. Chem Eng Technol 1997;20:617-23.

[6] Yu X, Tu ST, Wang Z, Qi Y. Development of a microchannel reactor concerning steam reforming of methanol. Chem Eng J 2006;116:123-32.

[7] Liu Y, Zhou W, Lin Y, Chen L, Chu X, Zheng T, et al. Novel copper foam with ordered hole arrays as catalyst support for methanol steam reforming microreactor. Appl Energy 2019;246:24-37.

[8] Parra-Cabrera C, Achille C, Kuhn S, Ameloot R. 3D printing in chemical engineering and catalytic technology: structured catalysts, mixers and reactors. Chem Soc Rev 2018;47:209-30.

[9] Li C, Yuan S, Yao X, Yu X, Li B, Tu ST. Structured nanoporous copper catalysts prepared by laser powder bed fusion and dealloying for on-board methanol steam reforming. Fuel 2023;347:128367.

[10] Hu S, Cui X, Yang L. Thermal matching characteristics in an autothermal methanol reforming microchannel reactor for hydrogen production. Chem Eng Sci 2023;280:118987.

[11] Zhang HJ, Xu C, Yu HY, Wu H, Jin F, Xiao F, et al. Enhancement of methanol steam reforming in a tubular fixed-bed reactor with simultaneous heating inside and outside. Energy 2022;254:124330.

[12] Wang G, Wang F, Li L, Zhang G. Experiment of catalyst activity distribution effect on methanol steam reforming performance in the packed bed plate-type reactor. Energy 2013;51:267-72.